ISSN 0915-633X

NATIONAL INSTITUTE FOR FUSION SCIENCE

3D Maxwell-Vlasov Boundary Value Problem Solution in Stellarator Geometry in Ion Cyclotron Frequency Range (final report)

V.L. Vdovin, T.Watari and A. Fukuyama

(Received - Oct. 28, 1996)

NIFS-469 Dec. 1996

RESEARCH REPORT
NIFS Series

NAGOYA, JAPAN

3D MAXWELL-VLASOV BOUNDARY VALUE PROBLEM SOLUTION in STELLARATOR GEOMETRY in ION CYCLOTRON FREQUENCY RANGE

(final report)

V. Vdovin (*), T.Watari

National Institute for Fusion Science, Nagoya

A.Fukuyama

Okayama University, Japan

(*) On leave from Kurchatov Institute of Atomic Energy, Moscow

October 1996

ABSTRACT

In this report we develop the theory for the wave excitation, propagation and absorption in 3-dimensional (3D) stellarator equilibrium high beta plasma in ion cyclotron frequency range (ICRF). This theory forms a basis for a 3D code creation, urgently needed for the ICRF heating scenarios development for the constructed LHD [1] and projected W7-X [2] stellarators and for the stellarators being at operation (like CHS, W7-AS, etc.). The theory solves the 3D Maxwell-Vlasov antenna-plasma-conducting shell boundary value problem in the non - orthogonal flux coordinates (ψ,θ,φ), ψ being magnetic flux function, θ and φ being the poloidal and toroidal angles, respectively. All basic physics, like wave refraction, reflection and diffraction are firstly self consistently included, along with the fundamental ion and ion minority cyclotron resonances, two ion hybrid resonance, electron Landau and TTMP absorption. Antenna reactive impedance and loading resistance are also calculated and urgently needed for an antenna -generator matching. This is accomplished in a real confining magnetic field being varying in a plasma major radius direction, in toroidal and poloidal directions, through making use of the hot dense plasma dielectric kinetic tensor.

We expand the solution in Fourier series over toroidal (φ) and poloidal (θ) angles and solve resulting ordinary differential equations in a radial like ψ - coordinate by finite difference method. The constructed discretization scheme is divergent - free one, thus retaining the basic properties of original equations. The Fourier expansion over angle coordinates has given to us the possibility to correctly construct the "parallel" wave number $k_{//}$ and thereby to correctly describe the ICRF waves absorption by a plasma.

The toroidal harmonics are tightly coupled with each other due to magnetic field inhomogenity of stellarators in toroidal direction. This is drastically different from axial symmetric plasma of the tokamaks. The inclusion in the problem major radius variation of magnetic field can strongly modify earlier results obtained for the straight helical, especially for high beta plasma, due to modification of locations of the two ion hybrid resonance layers. For W7-X like magnetic field topology the inclusion in our theory of a major radius inhomogenity of the magnetic field is a key element for correct description of RF power deposition profiles at all.

The theory is developed in a manner that includes tokamaks and magnetic mirrors as the particular cases through general metric tensor (provided by an equilibrium solver) treatment of the wave equations.

We describe the structure of newly developed stellarator ICRF 3D full wave code STELION, based on theory described in this report.

Key Words: Helical Device, stellarator, ICRF heating, metric tensor, Jacobian, equilibrium, antenna, Maxwell-Vlasov, tensor, toroidal coupling

Content

INTRODUCTION

The ion cyclotron resonance heating (ICRH) methods have proved to be useful for the bulk plasma heating and plasma production in small and middle size stellarators Recently good results for the ion and electron heating have been obtained on CHS [12] and W7-AS [13]. The ICRH methods are prepared for the newly constructed large helical LHD stellarator [1] and are planned for the projected W7-X advanced system stellarator [2]. It is well known that ICRF methods have achieved impressive results in large tokamaks like JET, TFTR, JT60-U, etc. The ICRH physics is well understood and there are several 2D full toroidal wave codes, describing major of RF phenomena in a tokamak plasma. In the stellarator plasma the confining magnetic field B_0 have a more complicated structure, mainly due to toroidal variation of B_0 (at least in classical machines). And tokamak-like 2D full wave toroidal codes are not applicable in the stellarators due to strong coupling of the toroidal harmonics. Such a coupling is absent in straight heliotrons and very useful results have been derived with the 2D codes making use the helical symmetry of a straight stellarator [3]. But additional major radius variation of B_0 in helical devices can be very important, especially in high beta plasma with the outside displaced magnetic surfaces, when the structure of the two ion hybrid resonance may be greatly modified [12].

In another class of advanced stellarators as W7-AS and W7-X the magnetic field topology is more closer to the tokamak B_0 topology, but again with the important feature of a space varying magnetic field strength in a toroidal direction, thus permitting the use also of specific non tokamak ICRF heating scenarios, like "magnetic beach" scenarios [4] In this last case the 2D full wave code [4], exploiting the toroidal inhomogenity of B_0, being useful in uderstanding of the "beach" scenarios in Advanced Systems, nevertheless suffers due to non inclusion of major radius variation of B_0

Thus for correct development of the ICRF heating scenarios in these new (and old) machines urgently needed is the development of three-dimensional (3D) ICRF code to provide the correct RF power deposition profiles to the electrons and ions, to rightly choose the position of ICRF antenna 1) high B_0 field side/low field side, 2) at what toroidal location an antenna must be placed; at $\omega < \omega_{ci}$ or at $\omega > \omega_{ci}$, etc. Of course such a code must be equipped by an appropriate kinetic plasma description (through the Vlasov-Landau kinetic equation) to include correctly the absorption and mode conversion mechanisms The 3D code will also provide the correct values of an antenna impedance , needed for an antenna type choice (low impedance or classic multi loop high impedance antenna) and its matching with a the RF generator.

In this report we developing the theory of a solution for the Maxwell-Vlasov boundary value problem in the ICRF range in a stellarator geometry. This theory must provide an algorithm for the creation of 3D code.

In section I we formulate the original ICRF full wave equations with the reduced order hot dielectric tensor. The section II is devoted to the stellarator equilibrium quantities like choice of the magnetic flux coordinates, evaluation of the metric tensor and B_0.The

method for the wave boundary value problem solution is developed in section III, where we derive the wave equations in non orthogonal flux coordinates system and solve them by Fourier expansion over the poloidal and toroidal angles and by finite differencing over a minor radius coordinate ψ.The advantage of the flux coordinates is that the wave equations contain only the first derivatives over the "radial" coordinate, thereby greatly simplifying the overall problem. The spatial differencing over the ψ coordinate we accomplish on the "semi-integer" mesh to provide the divergent-free discretization scheme, important to the ROTOR operators involved in a problem.

In section 4 we formulate the RF induced plasma currents in the orthogonal local coordinate system to use the simplest form of the dielectric tensor. Then we develop a procedure to formulate the currents in a chosen non orthogonal basic system. The boundary conditions for the electrical fields are established in sec.5, while appropriate form for the $k_{//}$ wave number , needed for the anti hermittian parts of tensor elements calculations (e.g., for absorption) is derived in section 6.

The loop antenna Fourier expanded RF excitation currents are given in sec.7, and local absorbed RF power expressions are formulated in sec 8. Structure of newly developed STELION code is described in sec.9. In the Appendix we derive the rotation matrix needed for transfer from the local orthogonal coordinate system to the basic non-orthogonal system.

1. *FULL WAVE EQUATION*

This report develops a 3D full wave calculation, which uses poloidal and toroidal harmonic expansions to solve the wave equation ($k_0 = \omega/c$, c - speed of light):

$$rotrot\vec{E} = \frac{4\pi i k_0}{c}(\vec{j}_p + \vec{j}^{ext}) + k_0^2 \vec{E} \qquad (1.1)$$

in flux coordinates with appropriate boundary conditions, in 3D stellarator geometry. In eq.(1.1) j^{ext} is an imposed antenna current density and j_p is the plasma current determined by the relation $\vec{j} = \vec{\sigma}\vec{E}$. In a strict description, $\vec{\sigma}$ represents the non local conductivity tensor [5] and eq.(1.1) takes the form of an integral equation. In this stage of investigation we assume, however, the local description in which induced plasma current in a chosen space point is determined by RF electrical field in the same space point.

We rewright the eq.(1.1) more compactly through the plasma dielectric tensor[10], $\vec{\varepsilon}$ as

$$rotrot\vec{E} = k_0^2 \vec{\varepsilon}\vec{E} + \frac{4\pi i k_0}{c}\vec{j}^{ext} \qquad \textbf{(1.1')}$$

The presented theory includes a full (non - perturbative) solution for longitudional electric field E and uses the reduced order form of the plasma dielectric tensor, to eliminate numerical problems with the resolution of very short wavelengths ion Bernstein waves at high phase velocities of the Fast Magnetosonic Waves (FW) $\omega / k_{\parallel} > v_{Te}$. It means that we simply install in finite ion Larmor radius expansion terms, proportional to the $(k_{\perp}\rho_i)^2$, the Alfvenian perpendicular wave number. That procedure rightly describes the absorbed RF power coming to the Bernstein waves [9]. At low phase velocities $\omega / k_{\parallel} < v_{Te}$ the finite Larmor radius corrections are insignificant ones and Fast Waves are converted to the kinetic Alfven waves (KAW) at $\omega < \omega_{ci}$ and this will be correctly described by our hot kinetic tensor description.

By solving the wave equation with appropriate boundary conditions in three dimensions (s, θ, φ), we will calculate the wave electric field E, the absorbed RF power profiles and driven in a plasma RF current if an antenna would be properly phased The poloidal and toroidal harmonic expansions allow variations in $k_{//}$ to be included correctly, while the minor radius, s, is treated by finite differencies Variations in the toroidal direction φ now can not be treated independently, as it does in tokamaks, but instead, in considered stellarator plasma case the toroidal and poloidal harmonics are tightly coupled by toroidal variation of confining magnetic field B_0, as well as by its major radius variation and by the non-circularity of the magnetic flux surfaces, and must be therefore be calculated simultaneously.

2. *EQUILIBRIUM AND FLUX COORDINATES*

One of most convenient methods applied to the theory of an equilibrium and plasma stability is the method of inverse mapping [6]. Making use of the flux coordinates significantly simplifies analytical calculations (due to $B \cdot \nabla s = 0$, $J \cdot \nabla s = 0$),and in simulations easily provides the needed precision of an established form and the relative positions of the magnetic surfaces. When developing the theory of solution of the Maxwell-Vlasov boundary value problem in Ion Cyclotron Frequency Range (ICRF) in a complicated 3-dimensional (3D) stellarator plasma we will use the flux coordinate system. Some complexity of making use such coordinates is related to the fact that these are not orthogonal But finally we will see that the results can be casted in compact and elegant form.

The magnetic field vector B in the plasma is written in a Clebsh represantation [8]

$$\vec{B} = \nabla s \times \nabla v, \tag{2.1}$$

where $s \in (0,1)$ is a radial flux variable (usually equal to the scaled toroidal flux $\psi(s)/\psi(1)$ in VMEC equilibrium code [7]) and $\nu \equiv \psi \times \theta - \chi \times \varphi + \lambda$, where θ is the poloidal angle, φ is the toroidal angle, $\lambda(s,\theta,\varphi)$ is a periodic stream function, and prime denotes d/ds. Here $2\pi\chi(s)$ is the poloidal magnetic flux. The contravariant components of B are then

$$\vec{B}\cdot\nabla s = 0,$$

$$\vec{B}\cdot\nabla\theta \equiv B^{\theta} = \left(\chi' - \lambda_{\varphi}\right)/J, \qquad (2.2)$$

$$\vec{B}\cdot\nabla\varphi \equiv B^{\varphi} = \left(\psi' + \lambda_{\theta}\right)/J,$$

where $J = \left(\nabla s\cdot\nabla\theta x\nabla\varphi\right)^{-1}$ is the Jacobian of the transformation between real space and flux coordinates $\vec{x} = \vec{x}(s,\theta,\varphi)$. Thus, elementary volume $dV = |J| ds d\theta d\varphi$ and plasma pressure p = p(s), where s = const is a radial coordinate labeling a magnetic flux surface. For nested toroidal surfaces, J never vanishes. In the case $\lambda = 0$, the magnetic field lines are straight in θ - φ coordinates, since $B^{\theta}/B^{\varphi} = \chi'/\psi' \equiv \iota(s)$, where ι is the rotational transform giving the mean pitch of the magnetic field lines

We need, for our goal, the contravariant basis vectors $\vec{e}^{\,i} \equiv \nabla x^{i}$, where $\vec{x} = (s,\theta,\varphi)$, and the covariant basis vectors $\vec{e}_i \equiv \partial\vec{r}/\partial x^{i} = J\vec{e}^{\,j} \times \vec{e}^{\,k}$, where (i,j,k) forms a positive triplet.

The all properties of internal geometry of the x^1, x^2, x^3 coordinate system are defined by an expression for the squared element length:

$$dl^2 = g_{ij}\,dx^{i}dx^{j}$$

The coefficients g_{ij} create the fundamental metric tensor and its elements are $g_{ij} = \vec{e}_i\vec{e}_j$. For the toroidal configuration under consideration, a cylindrical orthogonal system r = (R,Φ,Z) is appropriate, where R is the major radius, Φ is toroidal angle, and Z is the height above midplane (Fig.1). It then follows that the metric tensor elements are

$$g_{ij} = R_i R_j + R^2\Phi_i\Phi_j + Z_i Z_j$$

where $R_i = \partial R/\partial\alpha^{i}$, etc, and $(\alpha^1,\alpha^2,\alpha^3) = (s,\theta,\varphi)$. And another expression for the Jacobian is

$$J^2 = \det\left(G_{ij}\right),$$

$G_{ij} = \partial x_i/\partial\alpha^{j}$, where $(x_1,x_2,x_3) = (R,\Phi,Z)$.

In equilibrium solver VMEC code the dependence of R, Z and λ on the flux coordinate angles is expressed by Fourier series·

$$R = \sum R_{mn}(s)\cos(m\theta - n\varphi),$$

$$Z = \sum Z_{mn}(s)\sin(m\theta - n\varphi)\ , \qquad (2.3)$$

$$\lambda = \sum \lambda_{mn}(s)\sin(m\theta - n\varphi)$$

These series expansions in eq.(2.3) are used to evaluate the metric tensor elements, the Jacobian and the contravariant components of B - all being needed for a 3D ICRF code.

3. *NUMERICAL METHOD*

In above non-orthogonal system the variable A is expressed in terms of its covariant components·

$$\vec{A} = A_1\vec{e}^{\,1} + A_2\vec{e}^{\,2} + A_3\vec{e}^{\,3}$$

where

$$\vec{e}^{\,1} = \nabla\psi,\quad \vec{e}^{\,2} = \nabla\theta,\quad \vec{e}^{\,3} = \nabla\varphi$$

The eqs.(1.1) are then written in the flux coordinate system using the methods of tensor analysis This requires a knowledge of the elements of metric tensor whose elements are delivered by an equilibrium solver code.

The contrvariant components of ∇x∇xA are expressed as

$$rotrot\vec{A}\,|^1 = \frac{1}{J}\left\{\frac{\partial}{\partial x^2}\left[\frac{g_{31}}{J}\left(\frac{\partial A_3}{\partial x^2} - \frac{\partial A_2}{\partial x^3}\right) - \frac{g_{32}}{J}\left(\frac{\partial A_3}{\partial x^1} - \frac{\partial A_1}{\partial x^3}\right) + \frac{g_{33}}{J}\left(\frac{\partial A_2}{\partial x^1} - \frac{\partial A_1}{\partial x^2}\right)\right] - \right.$$

$$\left. \frac{\partial}{\partial x^3}\left[\frac{g_{21}}{J}\left(\frac{\partial A_3}{\partial x^2} - \frac{\partial A_2}{\partial x^3}\right) - \frac{g_{22}}{J}\left(\frac{\partial A_3}{\partial x^1} - \frac{\partial A_1}{\partial x^3}\right) + \frac{g_{23}}{J}\left(\frac{\partial A_2}{\partial x^1} - \frac{\partial A_1}{\partial x^2}\right)\right]\right\} \qquad (3.1)$$

Poloidal component is.

$$rotrot\vec{A}|^2 = -\frac{1}{J}\left\{\frac{\partial}{\partial x^1}\left[\frac{g_{31}}{J}\left(\frac{\partial A_3}{\partial x^2}-\frac{\partial A_2}{\partial x^3}\right)-\frac{g_{32}}{J}\left(\frac{\partial A_3}{\partial x^1}-\frac{\partial A_1}{\partial x^3}\right)+\frac{g_{33}}{J}\left(\frac{\partial A_2}{\partial x^1}-\frac{\partial A_1}{\partial x^2}\right)\right]-\right.$$

(3.2)

$$\left.\frac{\partial}{\partial x^3}\left[\frac{g_{11}}{J}\left(\frac{\partial A_3}{\partial x^2}-\frac{\partial A_2}{\partial x^3}\right)-\frac{g_{12}}{J}\left(\frac{\partial A_3}{\partial x^1}-\frac{\partial A_1}{\partial x^3}\right)+\frac{g_{13}}{J}\left(\frac{\partial A_2}{\partial x^1}-\frac{\partial A_1}{\partial x^2}\right)\right]\right\}$$

And toroidal component is as:

$$rotrot\vec{A}|^3 = \frac{1}{J}\left\{\frac{\partial}{\partial x^1}\left[\frac{g_{21}}{J}\left(\frac{\partial A_3}{\partial x^2}-\frac{\partial A_2}{\partial x^3}\right)-\frac{g_{22}}{J}\left(\frac{\partial A_3}{\partial x^1}-\frac{\partial A_1}{\partial x^3}\right)+\frac{g_{23}}{J}\left(\frac{\partial A_2}{\partial x^1}-\frac{\partial A_1}{\partial x^2}\right)\right]-\right.$$

(3.3)

$$\left.\frac{\partial}{\partial x^2}\left[\frac{g_{11}}{J}\left(\frac{\partial A_3}{\partial x^2}-\frac{\partial A_2}{\partial x^3}\right)-\frac{g_{12}}{J}\left(\frac{\partial A_3}{\partial x^1}-\frac{\partial A_1}{\partial x^3}\right)+\frac{g_{13}}{J}\left(\frac{\partial A_2}{\partial x^1}-\frac{\partial A_1}{\partial x^2}\right)\right]\right\}$$

In these equations J is the Jacobian of a system (x^1, x^2, x^3), in our case of the flux coordinate system (ψ, θ, φ):

$$J = \frac{1}{\nabla x^1\left[\nabla x^2 x \nabla x^3\right]} = \frac{1}{\nabla\psi\left[\nabla\theta x\nabla\varphi\right]}$$

3.2 *Fourier decomposition*

To solve eqs.(3.1)-(3.3) the electrical fields (E ≡ A) are expanded in Fourier series to describe their θ and φ dependencies. Since the equilibrium is not axis symmetric, the toroidal modes couple and can not be treated independently. Assuming that the equilibrium and the antenna generally are not up-down symmetrical about plane Z = 0, we expand the fields in series of the form:

$$A(\psi,\theta,\varphi) = \sum_{mn} a_{mn}(\psi)e^{i(m\theta+n\varphi)} \qquad (3.4)$$

The equilibrium quantities are varied in toroidal direction with the periodicity of the toroidal and/or helical coils, described for a concrete machine by the number N_P of a magnetic field periods. Respectively , we expand the equilibrium quantities in the double periodic Fourier series of the form:

$$g(\psi,\theta,\varphi) = \sum_{mn} g_{mn}(\psi) e^{i(m\theta + n N_p \varphi)} \qquad (3\,4')$$

Fourier analysis of eqs(3.1)-(3 3) then leads to the system of differencial equations in quasi radial coordinate, ψ These equations we will write below in explicit form The appearing convolution sums will be calculated by fast Fourier transform method.

We stress that due to double toroidal periodicity in stellarators the toroidal harmonics are coupled through the condition:

$$n' N_p + n - k = 0 \qquad (3\,4'')$$

being some kind analog of axis symmetry of tokamaks reflected to the stellarators.

3.3 *Spatial differencing*

After Fourier decomposition in θ and φ we set up a finite difference grid in ψ only. Critical moment for that descretization scheme is that for vector A, the identity div(rotA) = 0 must be hold identically by numerical difference operators. We state that RF induced current, rotrotA in eqs (3.1)-(3.3), is divergence free vector. Here we satisfy to that requirement introducing the mesh scheme, where we set up the system of non equally, in general, spaced "integer" surfaces with ψ_j , and a set of "half integer" surfaces, where $\psi_{j-1/2} = (\psi_j + \psi_{j-1})/2$. The integer surface j = 0 is defined as magnetic axis, while that with j = N is the conducting chamber, surrounding the plasma. We state, that covariant components a_θ and a_φ are defined on "integer" surfaces, while a_ψ is defined at the half points. Then contr variant components J^θ, J^φ of induced plasma currents (respectively, rotrotA) of derived vectors are centered at the "integer" surfaces, while the J^ψ (and rotrotA$|^\psi$) are centered at intermediate surfaces.

Now we install the expression eq.(3 4) into eqs.(3.1)-(3.3), assign plasma response and antenna currents in eq.(2.1) as being for brevity RHS, multiply both sides of equations by exp{-i(*l*θ+kφ) (*l and* k are integer numbers)and integrate over angles φ and θ. Then eqs.(3.1)-(3.3) are transformed into following equations. In psi direction (we changed ψ notation to s variable for simplicity):

$$\left(RHS^{(1)} J\right)_{lk} = \sum_{mn} \left\{ \left(-nl\left(\frac{g_{32}}{J}\right) + lm\left(\frac{g_{33}}{J}\right) + kn\left(\frac{g_{22}}{J}\right) - km\left(\frac{g_{23}}{J}\right) \right)_{l=m,(k-n):N_p} a_s^{mn}(s) +$$

$$\left(-ml\left(\frac{g_{31}}{J}\right)+km\left(\frac{g_{21}}{J}\right)\right)_{l-m,(k-n)/N_p} a_\theta^{mn}(s)+i\left(l\left(\frac{g_{33}}{J}\right)-k\left(\frac{g_{23}}{J}\right)\right)_{l-m,(k-n)/N_p}\frac{\partial a_\theta^{mn}}{\partial s}+$$

$$\left(-ml\left(\frac{g_{31}}{J}\right)+kn\left(\frac{g_{21}}{J}\right)\right)_{l-m,(k-n)/N_p} a_\varphi^{mn}(s)+i\left(-l\left(\frac{g_{32}}{J}\right)+k\left(\frac{g_{22}}{J}\right)\right)_{l-m,(k-n)/N_p}\frac{\partial a_\varphi^{mn}}{\partial s}\Big\} \quad \textbf{(3.5)}$$

In following two another equations we drop temporary the convolution indexes and m,n indexes for variables a_i. The equation for poloidal component of RHS is:

$$\left(RHS^{(2)}J\right)_{lk}=\sum_{mn}\Big\{\left(-kn\left(\frac{g_{12}}{J}\right)+km\left(\frac{g_{13}}{J}\right)\right)a_s+kn\left(\frac{g_{11}}{J}\right)a_\theta+ik\left(\frac{g_{13}}{J}\right)\frac{\partial a_\theta}{\partial s}-km\left(\frac{g_{11}}{J}\right)a_\varphi-ik\left(\frac{g_{12}}{J}\right)\frac{\partial a_\varphi}{\partial s}-$$

$$\frac{\partial}{\partial s}\left[\left(in\left(\frac{g_{23}}{J}\right)-im\left(\frac{g_{33}}{J}\right)\right)a_s-\left(in\frac{g_{31}}{J}\right)a_\theta+\left(\frac{g_{33}}{J}\right)\frac{\partial a_\theta}{\partial s}+\left(im\frac{g_{31}}{J}\right)a_\varphi-\left(\frac{g_{32}}{J}\right)\frac{\partial a_\varphi}{\partial s}\right]\Big\} \quad \textbf{(3.6)}$$

The toroidal component of RHS is:

$$\left(RHS^{(3)}J\right)_{lk}=\sum_{mn}\Big\{-\left(-nl\left(\frac{g_{12}}{J}\right)+lm\left(\frac{g_{13}}{J}\right)\right)a_s-l\left(n\frac{g_{11}}{J}\right)a_\theta-il\left(\frac{g_{13}}{J}\right)\frac{\partial a_\theta}{\partial s}+l\left(m\frac{g_{11}}{J}\right)a_\varphi+$$
$$il\left(\frac{g_{12}}{J}\right)\frac{\partial a_\varphi}{\partial s}+\frac{\partial}{\partial s}\left[\left(in\left(\frac{g_{22}}{J}\right)-im\left(\frac{g_{23}}{J}\right)\right)a_s-\left(in\frac{g_{21}}{J}\right)a_\theta+\left(\frac{g_{23}}{J}\right)\frac{\partial a_\theta}{\partial s}+\left(im\frac{g_{21}}{J}\right)a_\varphi-\left(\frac{g_{22}}{J}\right)\frac{\partial a_\varphi}{\partial s}\right]\Big\} \quad (3.7)$$

In these expressions it is understood that the left sides represent the (l,k) harmonic of plasma induced and antenna currents, while the right hand sides involve summing over all m and n. The coefficient in circle brackets refer the l - m, (k - n)/N_P convolution terms. With a_s defined at the half points and a_θ, a_φ at the integer points, we make use second order accurate centered difference formulae to derive:

$$\left(RHS^{(1)}J\right)^{lk}_{j+½}=\left(-nl(\bar{g}_{32})+lm(\bar{g}_{33})+kn(\bar{g}_{22})-km(\bar{g}_{23})\right)_{j+½}a^{(1)}_{j+½}+\left(nl(\bar{g}_{31})-kn(\bar{g}_{21})\right)_{j+½}\frac{a^{(2)}_{j+1}+a^{(2)}_{j}}{2}+$$

$$i\left(l\left(\bar{g}_{33}\right)-k\left(\bar{g}_{23}\right)\right)_{j+\frac{1}{2}}\left(\frac{a_{j+1}^{(2)}-a_{j}^{(2)}}{\Delta}\right)+\left(-lm\left(\bar{g}_{31}\right)+km\left(\bar{g}_{21}\right)\right)_{j+\frac{1}{2}}\frac{a_{j+1}^{(3)}+a_{j}^{(3)}}{2}+i\left(-l\left(\bar{g}_{32}\right)+k\left(\bar{g}_{22}\right)\right)_{j+\frac{1}{2}}\frac{a_{j+1}^{(3)}-a_{j}^{(3)}}{\Delta}$$

(**3.8)**

The discretized poloidal component is.

$$-\left(RHS^{(2)}J\right)_{j}^{lk}=-k\left(-n\left(\bar{g}_{12}\right)+m\left(\bar{g}_{13}\right)\right)_{j}\frac{a_{j+1/2}^{(1)}+a_{j-1/2}^{(1)}}{2}-k\left(n\left(\bar{g}_{11}\right)\right)_{j}a_{j}^{(2)}-ik\left(\bar{g}_{13}\right)_{j}\frac{a_{j+1}^{(2)}-a_{j-1}^{(2)}}{2\Delta}+$$

$$k\left(m\bar{g}_{11}\right)_{j}a_{j}^{(3)}+ik\left(\bar{g}_{12}\right)_{j}\frac{a_{j+1}^{(3)}-a_{j-1}^{(3)}}{2\Delta}-\frac{i}{\Delta}\left\{\left(-n\left(\bar{g}_{23}\right)+m\left(\bar{g}_{33}\right)\right)_{j+1/2}a_{j+1/2}^{(1)}-\left(-n\left(\bar{g}_{23}\right)+m\left(\bar{g}_{33}\right)\right)_{j-1/2}a_{j-1/2}^{(1)}\right\}$$

$$-\frac{i}{\Delta}\left\{\left(n\left(\bar{g}_{31}\right)\right)_{j+1/2}\frac{a_{j+1}^{(2)}+a_{j}^{(2)}}{2}-\left(n\left(\bar{g}_{31}\right)\right)_{j-1/2}\frac{a_{j}^{(2)}+a_{j-1}^{(2)}}{2}\right\}+\left\{\left(\bar{g}_{33}\right)_{j+1/2}\frac{a_{j+1}^{(2)}-a_{j}^{(2)}}{\Delta^{2}}-\left(\bar{g}_{33}\right)_{j-1/2}\frac{a_{j}^{(2)}-a_{j-1}^{(2)}}{\Delta^{2}}\right\}$$

$$+\left\{im\left(\bar{g}_{31}\right)_{j+1/2}\frac{a_{j+1}^{(3)}+a_{j}^{(3)}}{2\Delta}-\left(im\left(\bar{g}_{31}\right)\right)_{j-1/2}\frac{a_{j}^{(3)}+a_{j-1}^{(3)}}{2\Delta}\right\}+\left\{-\left(\bar{g}_{32}\right)_{j+1/2}\frac{a_{j+1}^{(3)}-a_{j}^{(3)}}{\Delta^{2}}+\left(\bar{g}_{32}\right)_{j-1/2}\frac{a_{j}^{(3)}-a_{j-1}^{(3)}}{\Delta^{2}}\right\}$$

(3.9)

The toroidal component is:

$$\left(RHS^{(3)}J\right)_{j}^{lk}=-l\left(-n\left(\bar{g}_{12}\right)+m\left(\bar{g}_{13}\right)\right)_{j}\frac{a_{j+1/2}^{(1)}+a_{j-1/2}^{(1)}}{2}-l\left(n\left(\bar{g}_{11}\right)\right)_{j}a_{j}^{(2)}-il\left(\bar{g}_{13}\right)_{j}\frac{a_{j+1}^{(2)}-a_{j-1}^{(2)}}{2\Delta}+l\left(m\left(\bar{g}_{11}\right)\right)_{j}a_{j}^{(3)}$$

$$+\ il\left(\bar{g}_{12}\right)_{j}\frac{a_{j+1}^{(3)}-a_{j-1}^{(3)}}{2\Delta}-\frac{i}{\Delta}\left\{\left(-n\left(\bar{g}_{22}\right)+m\left(\bar{g}_{23}\right)\right)_{j+1\ 2}a_{j+1/2}^{(1)}-\left(-n\left(\bar{g}_{22}\right)+m\left(\bar{g}_{23}\right)\right)_{j-1\ 2}a_{j-1/2}^{(1)}\right\}-$$

$$\frac{i}{\Delta}\left\{\left(n(\bar{g}_{21})\right)_{j+1/2}\frac{a_{j+1}^{(2)}+a_j^{(2)}}{2}-\left(n(\bar{g}_{21})\right)_{j-1/2}\frac{a_j^{(2)}+a_{j-1}^{(2)}}{2}\right\}+\left\{\left(\bar{g}_{23}\right)_{j+1/2}\frac{a_{j+1}^{(2)}-a_j^{(2)}}{\Delta^2}-\left(\bar{g}_{23}\right)_{j-1/2}\frac{a_j^{(2)}-a_{j-1}^{(2)}}{\Delta^2}\right\}$$

$$+\left\{\left(im(\bar{g}_{21})\right)_{j+1/2}\frac{a_{j+1}^{(3)}+a_j^{(3)}}{2\Delta}-\left(im(\bar{g}_{21})\right)_{j-1/2}\frac{a_j^{(3)}+a_{j-1}^{(3)}}{2\Delta}\right\}+\left\{-\left(\bar{g}_{22}\right)_{j+1/2}\frac{a_{j+1}^{(3)}-a_j^{(3)}}{\Delta^2}+\left(\bar{g}_{22}\right)_{j-1/2}\frac{a_j^{(3)}-a_{j-1}^{(3)}}{\Delta^2}\right\}$$

(3.10)

and hatted g is the g_{ik}/J. Again the right hand sides involve summing over all m and n. The coefficients in circle brackets refer the l - m,(k - n)/N_P convolution In these descretize equations for brevity we used indexes (1,2,3) instead of (s,θ,φ) terms.

Now it is to show that the above discretization scheme is divergent free one. The divergence of any vector A has a simple form for its contravariant components·

$$J div\vec{A}=\frac{\partial(JA^s)}{\partial s}+\frac{\partial(JA^\theta)}{\partial\theta}+\frac{\partial(JA^\varphi)}{\partial\varphi} \qquad (3.11)$$

and this is calculated by making use a centered difference scheme for the s (or ψ) derivative:

$$\frac{\partial(JA^s)}{\partial s}=\frac{(JA^s)_{j+1/2}-(JA^s)_{j-1/2}}{\Delta s}$$

So this is centered at the integer surface j, together with the θ and φ derivatives. Now we will calculate (3.11) making use the Eqs.(3.5)-(3.7). With a_φ defined at the semi mesh and a_θ at the integer mesh, we obtain (for simplicity $a_\varphi = 0$):

$$\left(\frac{\partial RHS^{(1)}J}{\partial s}\right)=\left(-nl(\bar{g}_{32})+lm(\bar{g}_{33})+kn(\bar{g}_{22})-km(\bar{g}_{23})\right)_{j+½}\left(\frac{a^{(1)}}{\Delta}\right)_{j+½}-$$

$$\left(-nl(\bar{g}_{32})+lm(\bar{g}_{33})+kn(\bar{g}_{22})-km(\bar{g}_{23})\right)_{j-½}\left(\frac{a^{(1)}}{\Delta}\right)_{j-½}+$$

$$\left(nl(\bar{g}_{31})-kn(\bar{g}_{21})\right)_{j+½}\left(\frac{a_{j+1}^{(2)}+a_{j}^{(2)}}{2\Delta}\right)-\left(nl(\bar{g}_{31})-kn(\bar{g}_{21})\right)_{j-½}\left(\frac{a_{j}^{(2)}+a_{j-1}^{(2)}}{2\Delta}\right)+$$

$$i\left(l(\bar{g}_{33})-k(\bar{g}_{23})\right)_{j+½}\left(\frac{a_{j+1}^{(2)}-a_{j}^{(2)}}{\Delta^2}\right)-i\left(l(\bar{g}_{33})-k(\bar{g}_{23})\right)_{j-½}\left(\frac{a_{j}^{(2)}-a_{j-1}^{(2)}}{\Delta^2}\right)+$$

$$\left(-lm(\bar{g}_{31})+km(\bar{g}_{21})\right)_{j+½}\left(\frac{a_{j+1}^{(3)}+a_{j}^{(3)}}{2\Delta}\right)-\left(-lm(\bar{g}_{31})+km(\bar{g}_{21})\right)_{j-½}\left(\frac{a_{j}^{(3)}+a_{j-1}^{(3)}}{2\Delta}\right)+$$

$$i\left(-l(\bar{g}_{32})+k(\bar{g}_{22})\right)_{j+½}\left(\frac{a_{j+1}^{(3)}-a_{j}^{(3)}}{\Delta^2}\right)-i\left(-l(\bar{g}_{32})+k(\bar{g}_{22})\right)_{j-½}\left(\frac{a_{j}^{(3)}-a_{j-1}^{(3)}}{\Delta^2}\right)$$

$$il\cdot RHS^{(2)}J=il\left(-kn(\bar{g}_{12})+km(\bar{g}_{13})\right)_{j}\left(\frac{a_{j+½}^{(2)}+a_{j-½}^{(2)}}{2}\right)+ilkn(\bar{g}_{11})_{j}a_{j}^{(2)}-$$

$$\frac{il}{\Delta}\left(\left(in(\bar{g}_{23})-im(\bar{g}_{33})\right)_{j+½}a_{j+½}^{(1)}-\left(in(\bar{g}_{23})-im(\bar{g}_{33})\right)_{j-½}a_{j-½}^{(1)}\right)+$$

$$\frac{il}{\Delta}\left(in(\bar{g}_{31})_{j+½}\left(\frac{a_{j+1}^{(2)}+a_{j}^{(2)}}{2}\right)-in(\bar{g}_{31})_{j-½}\left(\frac{a_{j}^{(2)}+a_{j-1}^{(2)}}{2}\right)\right)-$$

$$il\left((\bar{g}_{33})_{j+½}\left(\frac{a_{j+1}^{(2)}-a_{j}^{(2)}}{\Delta^2}\right)-(\bar{g}_{33})_{j-½}\left(\frac{a_{j}^{(2)}-a_{j-1}^{(2)}}{\Delta^2}\right)\right)+$$

$$il\left(ik(\bar{g}_{13})_{j}\frac{a_{j+1}^{(2)}-a_{j-1}^{(2)}}{2\Delta}\right)+il(-k)(m\bar{g}_{11})_{j}a_{j}^{(3)}$$

$$-il\left\{-im(\bar{g}_{31})_{j+½}\frac{a_{j+1}^{(3)}+a_{j}^{(3)}}{2\Delta}-im(\bar{g}_{31})_{j-½}\frac{a_{j}^{(3)}+a_{j-1}^{(3)}}{2\Delta}\right\}$$

$$-il\left\{-(\bar{g}_{32})_{j+½}\frac{a_{j+1}^{(3)}-a_{j}^{(3)}}{\Delta^2}+(\bar{g}_{32})_{j-½}\frac{a_{j}^{(3)}-a_{j-1}^{(3)}}{\Delta^2}\right\}$$

$$+(-ik)(il)(\bar{g}_{12})_{j}\frac{a_{j+1}^{(3)}-a_{j-1}^{(3)}}{2\Delta}$$

$$ik \cdot RHS^{(3)} J = ik\left(nl(\bar{g}_{12}) - lm(\bar{g}_{13})\right)_j \left(\frac{a^{(2)}_{j+½} + a^{(2)}_{j-½}}{2}\right) - ilkn(\bar{g}_{11})_j a_j^{(2)} +$$

$$\frac{ik}{\Delta}\left(\left(in(\bar{g}_{22}) - im(\bar{g}_{23})\right)_{j+½} a^{(1)}_{j+½} - \left(in(\bar{g}_{22}) - im(\bar{g}_{23})\right)_{j-½} a^{(1)}_{j-½}\right) -$$

$$\frac{ik}{\Delta} in\left((\bar{g}_{21})_{j+½}\left(\frac{a^{(2)}_{j+1} + a^{(2)}_{j}}{2}\right) - (\bar{g}_{21})_{j-½}\left(\frac{a^{(2)}_{j} + a^{(2)}_{j-1}}{2}\right)\right) +$$

$$ik\left((\bar{g}_{23})_{j+½}\left(\frac{a^{(2)}_{j+1} - a^{(2)}_{j}}{\Delta^2}\right) - (\bar{g}_{23})_{j-½}\left(\frac{a^{(2)}_{j} - a^{(2)}_{j-1}}{\Delta^2}\right)\right) +$$

$$kl(\bar{g}_{13})_j \frac{a^{(2)}_{j+1} - a^{(2)}_{j-1}}{2\Delta} + iklm(\bar{g}_{11})_j a^{(3)}_j$$

$$- kl(\bar{g}_{12})_j \frac{a^{(3)}_{j+1} - a^{(3)}_{j-1}}{2\Delta} +$$

$$ik\left\{im(\bar{g}_{21})_{j+½} \frac{a^{(3)}_{j+1} + a^{(3)}_{j}}{2\Delta} - im(\bar{g}_{21}) \frac{a^{(3)}_{j} + a^{(3)}_{j-1}}{2\Delta}\right\} +$$

$$ik\left\{-(\bar{g}_{22})_{j+½} \frac{a^{(3)}_{j+1} - a^{(3)}_{j}}{\Delta^2} + (\bar{g}_{22})_{j-½} \frac{a^{(3)}_{j} - a^{(3)}_{j-1}}{\Delta^2}\right\}$$

It is easily shown that by summing these discetized equations, the right hand side is canceled exactly. It means that the numerical divergence is identically zero. For a code goals it is clear, that in general it is necessary to interpolate quantities from one mesh to the other.

4. PLASMA RESPONSE

The RF induced currents are described by the dielectric tensor, the simplest famous form of which is realized in a special coordinate system with one axis directed along the total confining magnetic field vector B_0. So we temporary introduce such a system by choosing one of its unit vector to be coincident with $\nabla\psi$ direction, $e_s = \nabla s/|\nabla s|$, second unit vector e_h is directed parallel to the B_0, and the third vector is orthogonal to the first two vectors

$$\hat{e}_s = \frac{\nabla s}{|\nabla s|}, \qquad \hat{e}_h = \frac{\vec{B}_0}{|B_0|}, \qquad \hat{e}_b = \hat{e}_h \times \hat{e}_s$$

In this system the right hand side of basic equation (1.1), related to the plasma response, is written as

$$RHS = \frac{\nabla s}{|\nabla s|}(\bar{\varepsilon}_{11}E_s + \bar{\varepsilon}_{12}E_b + \bar{\varepsilon}_{13}E_h) + \hat{e}_b(\bar{\varepsilon}_{21}E_s + \bar{\varepsilon}_{22}E_b + \bar{\varepsilon}_{23}E_h) + \hat{e}_h(\bar{\varepsilon}_{31}E_s + \bar{\varepsilon}_{32}E_b + \bar{\varepsilon}_{33}E_h) \equiv$$

$$D_1\hat{e}_s + D_2\hat{e}_b + D_3\hat{e}_h \qquad (4.1)$$

We expand this vector over the covariant basis vectors

$$\alpha^1\hat{e}_1 + \alpha^2\hat{e}_2 + \alpha^3\hat{e}_3 = D_1\frac{\nabla s}{|\nabla s|} + D_2\hat{e}_b + D_3\hat{e}_h \qquad (4.1')$$

Multiplying consequently this equation by e_1 , e_2 and e_3 one obtains:

$$\|g_{ij}\| \begin{pmatrix} \alpha^1 \\ \alpha^2 \\ \alpha^3 \end{pmatrix} = \|\mu_{ij}\| \begin{pmatrix} D_1 \\ D_2 \\ D_3 \end{pmatrix} \qquad (4.2)$$

where matrix μ_{ij} is given in Appendix. And we find

$$\begin{pmatrix}\alpha^1\\ \alpha^2\\ \alpha^3\end{pmatrix} = \left\|g_{ij}^{-1}\right\| \bullet \left\|\mu_{ij}\right\| \begin{pmatrix}D_1\\ D_2\\ D_3\end{pmatrix} \tag{4.3}$$

From other hand we expand the electrical strength vector in the both coordinate systems (through the covariant components in non orthogonal system) as:

$$\vec{E} = A_1\hat{e}^1 + A_2\hat{e}^2 + A_3\hat{e}^3 =$$

$$\frac{E_s}{|\nabla s|}\nabla s + E_b\hat{e}_b + E_h\hat{e}_h$$

Multiplying again both sides by basic vectors e_1, e_2 and e_3, we expressed the connection of electrical field components in orthogonal system with the covariant field components in our non orthogonal coordinate system:

$$\begin{pmatrix}A_1\\ A_2\\ A_3\end{pmatrix} = \left\|\mu_{ij}\right\| \begin{pmatrix}E_s/|\nabla s|\\ E_b/|\nabla s|\\ E_h\end{pmatrix}, \qquad \begin{pmatrix}E_s\\ E_b\\ E_h|\nabla s|\end{pmatrix} = |\nabla s|\left\|\mu_{ij}^{-1}\right\| \begin{pmatrix}A_1\\ A_2\\ A_3\end{pmatrix}$$

Now the right hand side of eq.(1.1) can be written in a form:

$$k_0^2\vec{\varepsilon}\vec{E} = \left\|\hat{\varepsilon}_{ij}\right\| \begin{pmatrix}E_s\\ E_b\\ E_h|\nabla s|\end{pmatrix} = |\nabla s| \cdot \left\|\hat{\varepsilon}_{ij}\right\| \cdot \left\|\mu_{ij}^{-1}\right\| \begin{pmatrix}A_1\\ A_2\\ A_3\end{pmatrix} \equiv \begin{pmatrix}D_1\\ D_2\\ D_3\end{pmatrix}$$

where $\left\|\hat{\varepsilon}_{ij}\right\|$ is different from original $\left\|\bar{\varepsilon}_{ij}\right\|$ only due to $\left|\hat{\varepsilon}_{i3}\right| = \left\|\bar{\varepsilon}_{i3}\right\|/|\nabla s|$ The last equality in above equation gives now vector D and we install it in eq.(4.3) to obtain:

$$\begin{pmatrix}\alpha^1\\ \alpha^2\\ \alpha^3\end{pmatrix} = |\nabla s|\left\|g_{ij}^{-1}\right\| \cdot \left\|\mu_{ij}\right\| \cdot \left\|\bar{\varepsilon}_{ij}\right\| \cdot \left\|\mu_{ij}^{-1}\right\| \begin{pmatrix}A_1\\ A_2\\ A_3\end{pmatrix},$$

or in more compact form:

$$\begin{pmatrix} \alpha^1 \\ \alpha^2 \\ \alpha^3 \end{pmatrix} = \left\| \tilde{\varepsilon}_{ij} \right\| \begin{pmatrix} A_1 \\ A_2 \\ A_3 \end{pmatrix}$$

where "transformed" dielectric tensor in non orthogonal coordinate system has a form:

$$\left\| \tilde{\varepsilon}_{ij} \right\| = |\nabla s| \left\| g_{ij}^{-1} \right\| \cdot \left\| \mu_{ij} \right\| \cdot \left\| \hat{\varepsilon}_{ij} \right\| \cdot \left\| \mu_{ij}^{-1} \right\| \tag{4.5}$$

Finally the plasma contribution to the right side of eq.(2.1) looks very similar to cases for simple plasma geometries:

$$(RHS \bullet J) = J \bullet \left\| \tilde{\varepsilon}_{ij} \right\| \begin{pmatrix} A_1 \\ A_2 \\ A_3 \end{pmatrix} , \tag{4.6}$$

and respectively, in Fourier representation this looks like:

$$\left(RHS^{(1)} J\right)_j^{lk} = \sum_{mn} \left\{ \left(J\tilde{\varepsilon}_{11}\right)_{j+1/2}^{l-m,(k-n)/N_P} \frac{a_{j+1/2}^{(1)} + a_{j-1/2}^{(1)}}{2} + \left(J\tilde{\varepsilon}_{12}\right)_j^{l-m,(k-n)/N_P} a_j^{(2)} + \left(J\tilde{\varepsilon}_{13}\right)_j^{l-m,(k-n)/N_P} a_j^{(3)} \right\}$$

$$\left(RHS^{(2)} J\right)_j^{lk} = \sum_{mn} \left\{ \left(J\tilde{\varepsilon}_{21}\right)_j \frac{a_{j+1/2}^{(1)} + a_{j-1/2}^{(1)}}{2} + \left(J\tilde{\varepsilon}_{22}\right)_j a_j^{(2)} + \left(J\tilde{\varepsilon}_{23}\right)_j a_j^{(3)} \right\}$$

$$\left(RHS^{(3)} J\right)_j^{lk} = \sum_{mn} \left\{ \left(J\tilde{\varepsilon}_{31}\right)_j \frac{a_{j+1/2}^{(1)} + a_{j-1/2}^{(1)}}{2} + \left(J\tilde{\varepsilon}_{32}\right)_j a_j^{(2)} + \left(J\tilde{\varepsilon}_{33}\right) a_j^{(3)} \right\} \tag{4.7}$$

In the last two equations we dropped for simplicity the convolution indexes l-m,(n-k)/N_P.

5. *BOUNDARY CONDITIONS*

As usually we assume that the plasma is surrounded by perfectly conducting boundary of a machine vessel and between of them a vacuum layer (divertor region) is located. The imposed boundary condition at the last magnetic surface,

(j = N) coincident with the machine first wall is vanishing tangential electrical field:

$$\vec{E}\left(s = s_{wall}, \theta, \varphi\right)\Big|_{\tan g} = 0$$

It means that in a covariant wave field representation

$$\vec{A} = A_1 \nabla s + A_2 \nabla \theta + A_3 \nabla \varphi$$

the only non zero is the first (normal to a wall) term. We satisfy this requirement by keeping A_2=0 and A_3=0 for each Fourier harmonic j = M,N:

$$a_\theta^{mn} = 0, \quad a_\varphi^{mn} = 0$$

To derive boundary conditions at the magnetic axis ($\psi \equiv s = 0$) by a simplest way we make use analogy with the analytical solution for a plasma cylinder with homogeneous density (near of magnetic axis this is a good approximation). In this case longitudinal component of wave electric and magnetic fields is expressed through the Bessel functions of order m:

$$E_\varphi = E_0 J_m(k_\perp s) e^{i(m\theta + n\varphi)}$$

And we use its asymptotic behavior to derive the φ - component asymptotic when s ($\equiv\psi$) $\to$0:

$$a_\varphi = s^{|m|}(\nu_1 + \nu_2 s^2 + \ldots)$$

The transverse electrical fields are expressed through the Bessels and their first radial derivatives. So it easy to derive asymptotic behavior of the covariant s - and θ components of E:

$$a_s = s^{|m|-1}\left(\nu_3 + \nu_4 s^2 + \ldots\right)$$

$$a_\theta = s^{|m|-1}(\nu_5 s + \nu_6 s^3 + \ldots)$$

The only the θ - and φ - components of A are required at the axis s = 0, one has

$$a_\theta^{mn} = 0 \quad , \text{ all m and n,}$$

$$a_\varphi^{mn} = 0 \qquad \text{if } m \neq 0,$$

$$\frac{\partial a_\varphi^{mn}}{\partial s} = 0 \quad \text{if } m = 0$$

Now boundary conditions have been established.

6. *PARALLEL WAVE NUMBER*

The plasma dielectric tensor $\tilde{\varepsilon}(s,\theta,k_\parallel^{mn})$, appearing in eq (4.7), depends on $k_\parallel^{mn}$ through plasma dispersion function $Z((\omega - N\Omega_{ce,i})/k_{//}^{mn}v_{Te,i})$, where N is the cyclotron harmonic number. To account the effect of the poloidal magnetic field influence on $k_{//}$ wave number formation it is usually considered that the $k_{//}$ is the component of the spatial gradient in the direction of B_0. The gradient operator in a non orthogonal system is

$$\nabla = \nabla s \frac{\partial}{\partial s} + \nabla\theta \frac{\partial}{\partial\theta} + \nabla\varphi \frac{\partial}{\partial\varphi}$$

And we define $k_{//}$ as.

$$ik_\parallel = \hat{e}_h \bullet \nabla = \hat{e}_h (\nabla\theta \frac{\partial}{\partial\theta} + \nabla\varphi \frac{\partial}{\partial\varphi})$$

Expanding $\hat{e}_h$ over unit vectors e_φ and e_θ

$$\hat{e}_h = \hat{e}_\varphi \frac{B^\varphi}{|B|} + \hat{e}_\theta \frac{B^\theta}{|B|} \qquad (6\ 1)$$

Finally we have

$$k_\parallel = n\frac{B^\varphi}{|B|} + m\frac{B^\theta}{|B|} \qquad (6.2)$$

where

$$|B|^2 \equiv B^i B_i = (B^\theta)^2 g_{22} + 2B^\theta B^\varphi g_{23} + (B^\varphi)^2 g_{33}$$

This equation (6.2) generalizes the $k_{//}$ definition for a stellarator magnetic field geometry. The tokamak $k_{//}$ case is easily obtained from eq.(6.2). In this equation (6.2) the poloidal field dominates the $k_{//}$ variation when

$$|m| \geq n \frac{B^\varphi}{B^\theta}$$

7. *ANTENNA AND ITS FOURIER SPECTRA*

As a starting point we consider a single loop classical antenna exciting into plasma the Fast Waves. The antenna is fed by two radial feeders. The imposed RF antenna current follows antenna's magnetic surface at $s = s_{ant}$ and flows poloidally and radially in short end parts of the loop (Fig.2). The poloidal distribution of antenna poloidal current density is given by

$$j_\theta(s = s_{ant}, \theta, \varphi) = j_0(\varphi)\cos(\beta\theta)$$

and the poloidal variation of the radial currents, $j_s(\theta)$, is given by delta function $\delta(\theta \pm \theta_a)$.

The poloidal antenna extension is $2\theta_a$, the maximal toroidal broadness of an antenna is D. The toroidal variation (in coordinate φ) of an antenna current is assumed to be absent (its dependence over φ angle is a step function with a base equal D).

We expand these current density distributions in the Fourier series:

$$j_\theta(\theta, \varphi) = \sum_{mn} J_\theta^{mn} e^{i(m\theta + \varphi n)} \delta(s - s_a) \ ,$$

$$j_s(s, \theta, \varphi) = \sum_{mn} J_s^{mn}(s) e^{i(m\theta + n\varphi)}$$

Simple calculations give

$$J_\theta^{mn} = \frac{J_0}{4\pi^2 R}\cdot\frac{\sin(n\varphi_a)}{n\varphi_a}\left[\frac{\sin(m+\beta)\theta_a}{m+\beta}+\frac{\sin(m-\beta)\theta_a}{m-\beta}\right]$$

$$J_s^{mn}(s) = i\frac{J_0\cos(\beta\theta_a)}{4\pi^2 R}\sin(m\theta_a)\frac{\sin(n\varphi_a)}{n\varphi_a}\cdot\frac{s_a}{s}$$

$$J_\varphi^{mn}(s) = J_s^{mn}(s)\sin(\alpha)$$

where angle α is due to non orthoganality

$$\sin(\alpha) = \frac{\nabla s\cdot\nabla\varphi}{|\nabla s||\nabla\varphi|} = \frac{R}{J^2}\left(g_{12}g_{23}-g_{22}g_{13}\right)\frac{1}{|\nabla s|}$$

Here $R=R_0 + a\cos\theta_a$, a is a plasma minor radius at equatorial plane and J_0 - total antenna loop current at the middle of the loop. In the expression for $\sin(\alpha)$ metric elements, $|\nabla s|$ and Jacobian J may be evaluated reasonably at $s=s_{ant}$ and $\theta=\theta_{ant}$.

These formulas can be readily extended to toroidal multi loop arrays with an imposed loops phasing.

8. *ABSORBED RF POWER*

The total absorbed and mode converted RF power is given by

$$P(s,\theta,\varphi) = \frac{1}{2}\mathrm{Re}(\vec{E}^*\cdot\vec{j}_p)$$

The plasma current density, induced by RF waves, is expressed as

$$\vec{j}_p(s,\theta,\varphi) = \sum_{mn}\vec{\sigma}(s,\theta,\varphi,k_\parallel^{mn})\vec{E}_{mn}(s)e^{i(m\theta+n\varphi)}$$

and we have

$$P(s,\theta,\varphi) = \frac{\omega}{8\pi} \mathrm{Re} \sum_{mn} \vec{E}^{*}_{mn}(s) \tilde{\varepsilon}^{a}(s,\theta,\varphi,k_{\parallel}^{mn}) \vec{E}_{mn}(s) \qquad (8.1)$$

where we introduced dielectric tensor $\tilde{\varepsilon} = 4\pi i / \omega\tilde{\sigma} + \tilde{I}$ and $\tilde{\varepsilon}^{a}$ is anti hermittian part of this tensor.

If a multi loop antenna is properly phased and radiates some traveling Fast Waves, the RF power, absorbed by the electrons, drives in toroidal direction some current which is readily evaluated by

$$J_{cd}(s,\theta) = \left\langle \frac{19.2 \times 10^{15}}{\Lambda} \cdot \frac{kT_e}{n_e} \cdot \frac{\hat{j}_d}{\hat{p}_d} P(s,\theta,\varphi) \right\rangle_{\varphi} \qquad \mathbf{(8.2)}$$

where the angular brackets mean average over toroidal angle φ. The normalized current drive efficiency j_d/p_d is a strong function of the local parallel phase velocity $u = v_{//}/v_{Te} = \omega/k_{//}v_{Te}$. This is given in [11].

In stellarators usually needs for the RF driven currents are small ones: they may be needed for a compensation of some unwanted equilibrium currents or to compensate possible driven currents produced by NB heating.

9. STRUCTURE OF THE STELION CODE

STELION is constructed as a boundary value problem code. The notation and layot follow strictly to the standarts and conventions of usual methodology to ensure that program is readily understood and easily trasferred from one computer to another. Mnemonic variable names correspond closely to the notation used in this report and the program file contains indexes of all subroutines, COMMON blocks and variables used throughout the code. No extended library is required, the packet of subroutines for a complex matrix inversion is included. Here we use compact pointer storage method [14].

The most effort is expended in initialization since the matrix of block bands diagonal system is calculated only once. Fig.3 shows the calling sequence in STELION. Equilibrium date is input, using the format of the VMEC code, in WOUT file. This data is used to construct the metric tensor and other coefficients in METRIN . Splines technic is used to transfer this equilibrium metric from VMEC flux coordinate mesh ("radial") to fine flux mesh, required for a treatment of small scale Fast waves and smaller scale converted waves (in present version of STELION code - kinetic Alfven waves, important for a treatment of "Heivy" minority ions scenario and "magnetic beach" scenario) in IC frequency range.

This is accomplished in METRIC Then metric elements and another coefficients are consequently replaced by their Fourier transforms in FOURT1

On a basis of these fine quantities the kinetic tensor ε_{ij} is calculated in TENSOR, and again it consequently replaced by their Fourier transforms in FOURT2 The vectorization procedure is used in the code because these transforms are possible to do independently on each radial (flux coordinate) mesh position. To construct basic matrix, descibing wave processes, are used 21 functions, RRIP, RFI, ..., ZZIP, describing the coefficients in descretized equations and accumulating an information on metric, Jacobian and kinetic tensor. Using these functions nonzero elements of the matrix are constructed in MATR.

Fourier transformed antenna currents are calculated in RIGHT. To correctly describe toroidal component of the exciting currents some information on a metric is needed from METRIC. This provides a right hand side of complex linear system Ax = b. This system is solved in SOLVER making use a compact pointer storage method. The found electrical fields X, together with the kinetic tensor from FOURT2, are used to calculate space RF power deposition profiles to ions and electrons, as well as as an antenna complex impedance (neede for a mathcing with RF generator) and its toroidal and poloidal spectrums, in POWER. Output information and plotting are provided by OUT subroutine.

APPENDIX

Calculation of matrix Mu.

In this section we derive the rotation matrix connecting the covariant components A_i of an electrical vector with the (E_s, E_b, E_h) components of the same vector in (s, b, h) orthogonal coordinate system introduced in sec.4. The h- coordinate of orthogonal local system is along a total magnetic magnetic field

$$\vec{B} = B^{\theta}\hat{e}_{\theta} + B^{\varphi}\hat{e}_{\varphi} \tag{A1}$$

and unit vector directed along the B_0 is

$$\hat{e}_h = \vec{B}/|\vec{B}| = B^{\theta} / B\hat{e}_{\theta} + B^{\varphi} / B\hat{e}_{\varphi} \equiv c_1\hat{e}_3 + c_2\hat{e}_2$$

where the total local confining magnetic field is given by

$$|B|^2 \equiv B^i B_i = \left(B^\theta\right)^2 g_{22} + 2B^\theta B^\varphi g_{23} + \left(B^\varphi\right)^2 g_{33}$$

We recall that, for example,

$$g_{22} = \hat{e}_2 \cdot \hat{e}_2 = \left(\frac{\partial \vec{r}}{\partial \theta}\right)^2$$

Multiplying the eq.(4.4) by covariant basis vector e_1 , one has

$$A_1 = \frac{E_s}{|\nabla S|} + E_b \hat{e}_1 \left[\hat{e}_h \times \hat{e}_s\right] + E_h \hat{e}_1 \cdot \hat{e}_h$$

Opening the vector product as

$$\hat{e}_1 [\hat{e}_h \hat{e}^1] = -\frac{1}{J}\left[c_1\left(g_{23}g_{13} - g_{12}g_{33}\right) + c_2\left(g_{22}g_{13} - g_{12}g_{23}\right)\right]$$

etc., multiplying again by e_2 and e_3, one obtains

$$\left|\mu_{ij}\right| = \begin{pmatrix} \ldots 1 \ldots & -\frac{1}{J}\left[c_1\left(g_{13}g_{23} - g_{12}g_{33}\right) + c_2\left(g_{13}g_{22} - g_{12}g_{23}\right)\right] & \ldots\ldots c_1 g_{13} + c_2 g_{12} \\ \ldots 0 \ldots\ldots\ldots & -\frac{1}{J}c_1\left(g_{23}^2 - g_{22}g_{33}\right) & \ldots\ldots\ldots c_1 g_{23} + c_2 g_{22} \\ \ldots 0 \ldots\ldots\ldots & -\frac{1}{J}c_2\left(g_{22}g_{33} - g_{23}^2\right) & \ldots\ldots\ldots c_1 g_{33} + c_2 g_{23} \end{pmatrix}$$

This matrix is installed in eq.(4.2) and to following formulas.

References

1 A Iiyoshi, M Fujiwara, O Motojima, N.Ohybu, K.Yamazaki

Fusion Technology 17(1990) 169

2 WENDELSTEIN project Group, IPP-EURATOM Association,
WENDELSTEIN 7-X, Phase II, Application for Preferencial Support, June 1994

3 A.Fukuyama, N.Okazaki, A.Goto, S.Itoh,K.Itoh, Nuclear Fusion 26(1986)151

4 V.Vdovin, ICRF magnetic beach scenarios in stellarators W7-AS and W7-X

IPP report, May 1995

5. V.P.Silin, A.Rukhadze, Electrodynamic of Plasma and Like Plasma Media,

Nauka, Moscow 1961

6. J.M.Green, J.L.Johnson, K.E.Weimer, Physics of Fluids 24(1981)14

7. S.Hirshman, J.Witson, Physics of Fluids 26(12) 1983

8 F Bauer, O Betancurt, P.Garabedian, A computational method in Plasma

Physics (Springer - Verlag, New-York, 1978)

9. D.Smithe, P.Colestock, R Kammash, R.Kashuba, Nuclear Fusion 27(1987) 1319

10. A Akhiezer et al, "Plasma Electrodynamics" (Publisher: "Science",
Moscow,1974

11. D.Ehst, C.Karney, Nuclear Fusion 31(1991) 1933

12. CHS ICRF heating results, Submitted to Nucl. Fus. (1996)
13. Recent W7-AS ICRF results, Oak-Ridge Stellarator News, 1996

Fig.1 Cylindrical and Local coordinate systems

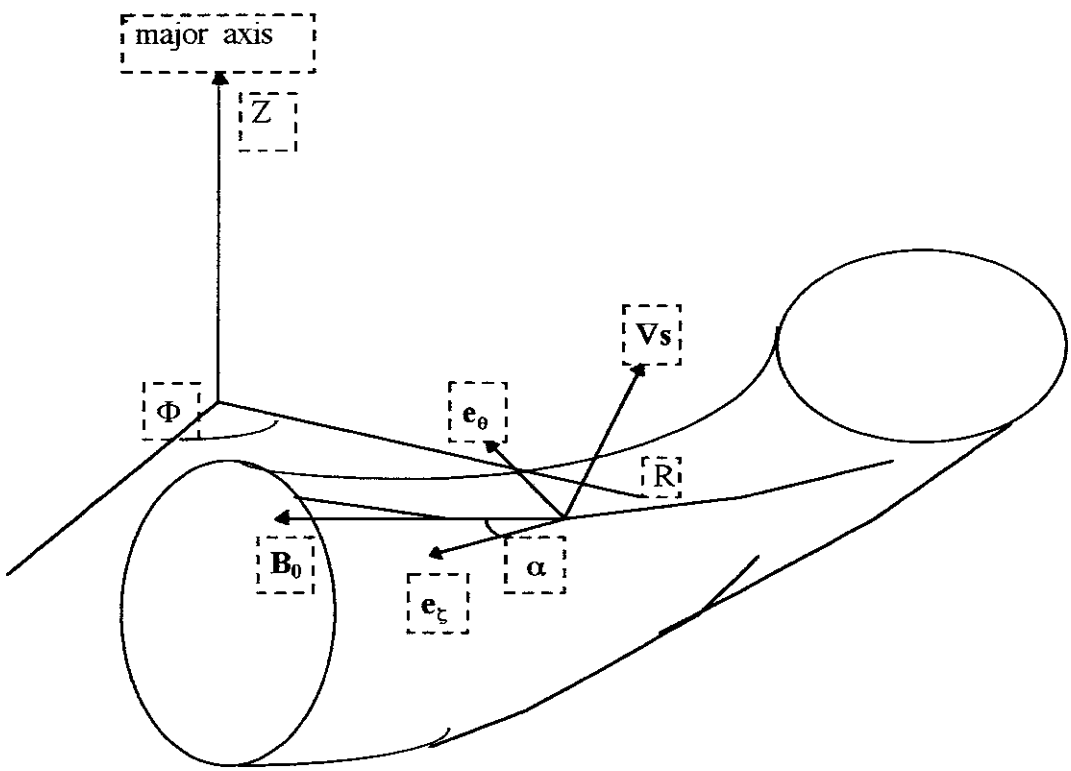

Fig.2 Dimensions of an individual antenna loop

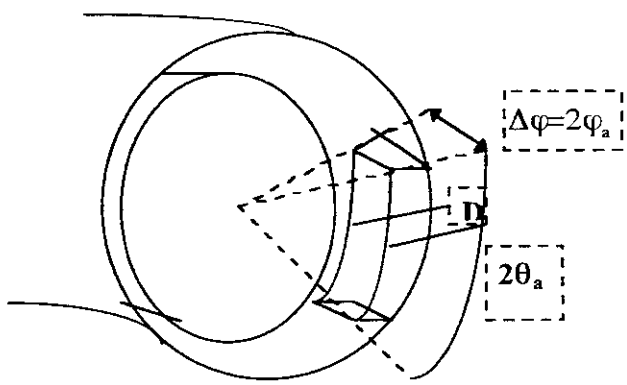

Fig. 3 Subroutine calling sequencies (3D ICRF STELION code)

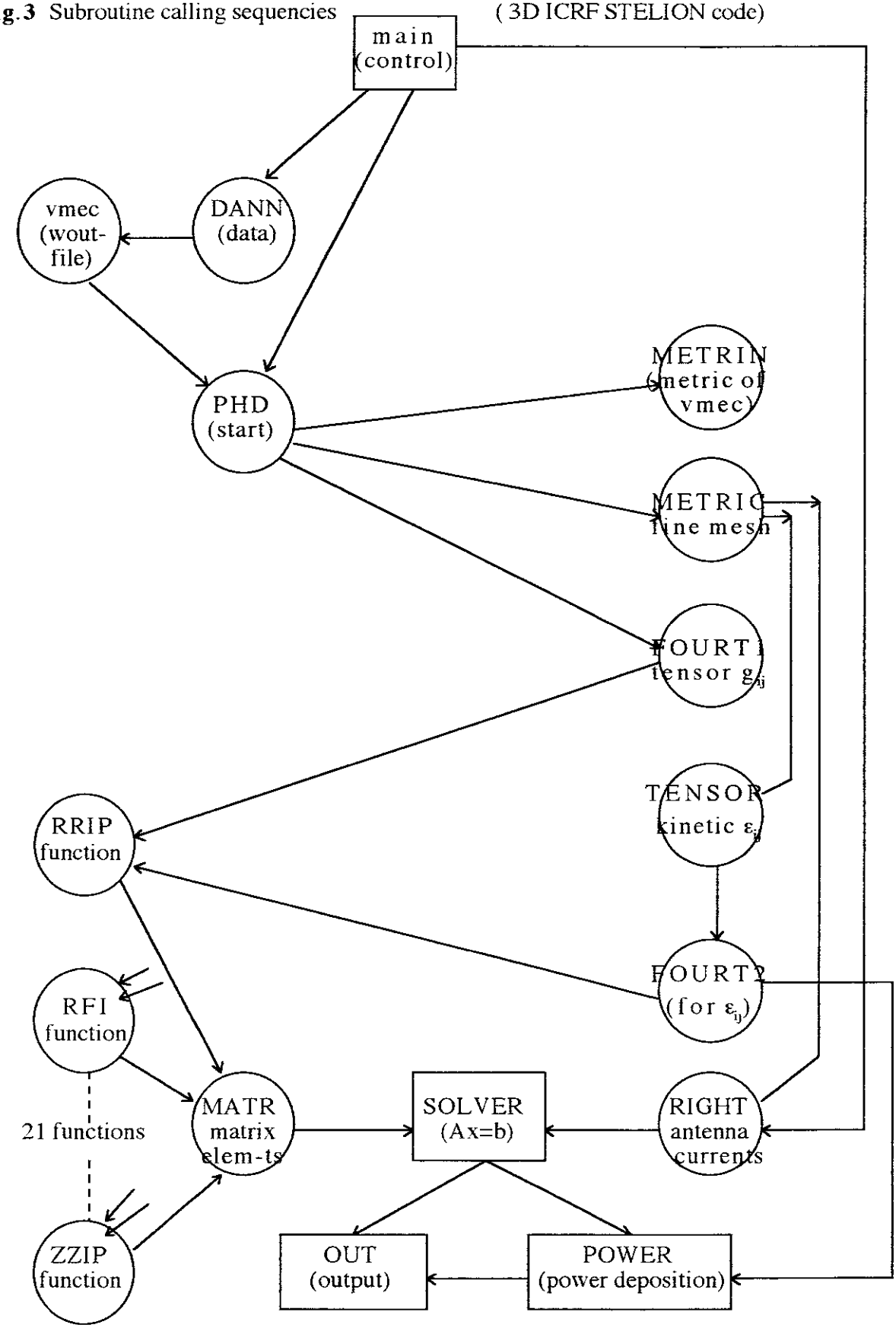

Recent Issues of NIFS Series

NIFS-431 K. Tsuzuki, M. Natsir, N Inoue, A. Sagara, N. Noda, O Motojima, T. Mochizuki, T. Hino and T. Yamashina,
Hydrogen Absorption Behavior into Boron Films by Glow Discharges in Hydrogen and Helium; Aug. 1996

NIFS-432 T.-H. Watanabe, T. Sato and T. Hayashi,
Magnetohydrodynamic Simulation on Co- and Counter-helicity Merging of Spheromaks and Driven Magnetic Reconnection; Aug. 1996

NIFS-433 R. Horiuchi and T. Sato,
Particle Simulation Study of Collisionless Driven Reconnection in a Sheared Magnetic Field; Aug. 1996

NIFS-434 Y. Suzuki, K. Kusano and K. Nishikawa,
Three-Dimensional Simulation Study of the Magnetohydrodynamic Relaxation Process in the Solar Corona. II.; Aug. 1996

NIFS-435 H. Sugama and W. Horton,
Transport Processes and Entropy Production in Toroidally Rotating Plasmas with Electrostatic Turbulence; Aug. 1996

NIFS-436 T. Kato, E. Rachlew-Källne, P. Hörling and K.-D Zastrow,
Observations and Modelling of Line Intensity Ratios of OV Multiplet Lines for 2s3s 3S1 - 2s3p 3Pj; Aug. 1996

NIFS-437 T. Morisaki, A. Komori, R. Akiyama, H. Idei, H. Iguchi, N. Inoue, Y. Kawai, S. Kubo, S. Masuzaki, K. Matsuoka, T. Minami, S. Morita, N. Noda, N. Ohyabu, S. Okamura, M. Osakabe, H. Suzuki, K. Tanaka, C. Takahashi, H. Yamada, I. Yamada and O. Motojima,
Experimental Study of Edge Plasma Structure in Various Discharges on Compact Helical System; Aug. 1996

NIFS-438 A. Komori, N. Ohyabu, S. Masuzaki, T. Morisaki, H. Suzuki, C. Takahashi, S. Sakakibara, K. Watanabe, T. Watanabe, T. Minami, S. Morita, K. Tanaka, S. Ohdachi, S. Kubo, N. Inoue, H. Yamada, K. Nishimura, S. Okamura, K. Matsuoka, O. Motojima, M. Fujiwara, A. Iiyoshi, C. C. Klepper, J.F. Lyon, A.C. England, D.E. Greenwood, D.K. Lee, D.R. Overbey, J.A. Rome, D.E. Schechter and C.T. Wilson,
Edge Plasma Control by a Local Island Divertor in the Compact Helical System; Sep. 1996 (IAEA-CN-64/C1-2)

NIFS-439 K. Ida, K. Kondo, K. Nagaski T. Hamada, H. Zushi, S. Hidekuma, F. Sano, T. Mizuuchi, H. Okada, S. Besshou, H. Funaba, Y. Kurimoto, K. Watanabe and T. Obiki,
Dynamics of Ion Temperature in Heliotron-E; Sep. 1996 (IAEA-CN-64/CP-5)

NIFS-440 S. Morita, H. Idei, H. Iguchi, S. Kubo, K. Matsuoka, T. Minami, S. Okamura, T.

Ozaki, K. Tanaka, K. Toi, R. Akiyama, A. Ejiri, A. Fujisawa, M. Fujiwara, M. Goto, K. Ida, N. Inoue, A. Komori, R. Kumazawa, S. Masuzaki, T. Morisaki, S. Muto, K. Narihara, K. Nishimura, I. Nomura, S. Ohdachi, M.. Osakabe, A. Sagara, Y. Shirai, H. Suzuki, C. Takahashi, K. Tsumori, T. Watari, H. Yamada and I. Yamada,
A Study on Density Profile and Density Limit of NBI Plasmas in CHS; Sep. 1996 (IAEA-CN-64/CP-3)

NIFS-441 O. Kaneko, Y. Takeiri, K. Tsumori, Y. Oka, M. Osakabe, R. Akiyama, T. Kawamoto, E. Asano and T. Kuroda,
Development of Negative-Ion-Based Neutral Beam Injector for the Large Helical Device; Sep. 1996 (IAEA-CN-64/GP-9)

NIFS-442 K. Toi, K.N. Sato, Y. Hamada, S. Ohdachi, H. Sakakita, A. Nishizawa, A. Ejiri, K. Narihara, H. Kuramoto, Y. Kawasumi, S. Kubo, T. Seki, K. Kitachi, J. Xu, K. Ida, K. Kawahata, I. Nomura, K. Adachi, R. Akiyama, A. Fujisawa, J. Fujita, N. Hiraki, S. Hidekuma, S. Hirokura, H. Idei, T. Ido, H. Iguchi, K. Iwasaki, M. Isobe, O. Kaneko, Y. Kano, M. Kojima, J. Koog, R. Kumazawa, T. Kuroda, J. Li, R. Liang, T. Minami, S. Morita, K. Ohkubo, Y. Oka, S. Okajima, M. Osakabe, Y. Sakawa, M. Sasao, K. Sato, T. Shimpo, T. Shoji, H. Sugai, T. Watari, I. Yamada and K. Yamauti,
Studies of Perturbative Plasma Transport, Ice Pellet Ablation and Sawtooth Phenomena in the JIPP T-IIU Tokamak; Sep. 1996 (IAEA-CN-64/A6-5)

NIFS-443 Y. Todo, T. Sato and The Complexity Simulation Group,
Vlasov-MHD and Particle-MHD Simulations of the Toroidal Alfvén Eigenmode; Sep. 1996 (IAEA-CN-64/D2-3)

NIFS-444 A. Fujisawa, S. Kubo, H. Iguchi, H. Idei, T. Minami, H. Sanuki, K. Itoh, S. Okamura, K. Matsuoka, K. Tanaka, S. Lee, M. Kojima, T.P. Crowley, Y. Hamada, M. Iwase, H. Nagasaki, H. Suzuki, N. Inoue, R. Akiyama, M. Osakabe, S. Morita, C. Takahashi, S. Muto, A. Ejiri, K. Ida, S. Nishimura, K. Narihara, I. Yamada, K. Toi, S. Ohdachi, T. Ozaki, A. Komori, K. Nishimura, S. Hidekuma, K. Ohkubo, D.A. Rasmussen, J.B. Wilgen, M. Murakami, T. Watari and M. Fujiwara,
An Experimental Study of Plasma Confinement and Heating Efficiency through the Potential Profile Measurements with a Heavy Ion Beam Probe in the Compact Helical System; Sep. 1996 (IAEA-CN-64/C1-5)

NIFS-445 O. Motojima, N. Yanagi, S. Imagawa, K. Takahata, S. Yamada, A. Iwamoto, H. Chikaraishi, S. Kitagawa, R. Maekawa, S. Masuzaki, T. Mito, T. Morisaki, A. Nishimura, S. Sakakibara, S. Satoh, T. Satow, H. Tamura, S. Tanahashi, K. Watanabe, S. Yamaguchi, J. Yamamoto, M.Fujiwara and A. Iiyoshi,
Superconducting Magnet Design and Construction of LHD; Sep. 1996 (IAEA-CN-64/G2-4)

NIFS-446 S. Murakami, N. Nakajima, S. Okamura, M. Okamoto and U. Gasparino,
Orbit Effects of Energetic Particles on the Reachable β–Value and the Radial Electric Field in NBI and ECR Heated Heliotron Plasmas; Sep. 1996 (IAEA-CN-64/CP -6) Sep. 1996

NIFS-447 K. Yamazaki, A. Sagara, O. Motojima, M. Fujiwara, T. Amano, H. Chikaraishi, S. Imagawa, T. Muroga, N. Noda, N. Ohyabu, T. Satow, J.F. Wang, K.Y. Watanabe, J. Yamamoto , H. Yamanishi, A. Kohyama, H. Matsui, O. Mitarai, T. Noda, A.A. Shishkin, S. Tanaka and T. Terai
Design Assessment of Heliotron Reactor; Sep. 1996 (IAEA-CN-64/G1-5)

NIFS-448 M. Ozaki, T. Sato and the Complexity Simulation Group.
Interactions of Convecting Magnetic Loops and Arcades; Sep. 1996

NIFS-449 T. Aoki,
Interpolated Differential Operator (IDO) Scheme for Solving Partial Differential Equations; Sep. 1996

NIFS-450 D. Biskamp and T. Sato,
Partial Reconnection in the Sawtooth Collapse; Sep. 1996

NIFS-451 J. Li, X. Gong, L. Luo, F.X. Yin, N. Noda, B. Wan, W. Xu, X. Gao, F. Yin, J.G. Jiang, Z. Wu., J.Y. Zhao, M. Wu, S. Liu and Y. Han,
Effects of High Z Probe on Plasma Behavior in HT-6M Tokamak; Sep. 1996

NIFS-452 N. Nakajima, K. Ichiguchi, M. Okamoto and R.L. Dewar,
Ballooning Modes in Heliotrons/Torsatrons; Sep. 1996 (IAEA-CN-64/D3-6)

NIFS-453 A. Iiyoshi,
Overview of Helical Systems; Sep. 1996 (IAEA-CN-64/O1-7)

NIFS-454 S. Saito, Y. Nomura, K. Hirose and Y.H. Ichikawa,
Separatrix Reconnection and Periodic Orbit Annihilation in the Harper Map; Oct. 1996

NIFS-455 K. Ichiguchi, N. Nakajima and M. Okamoto,
Topics on MHD Equilibrium and Stability in Heliotron / Torsatron; Oct. 1996

NIFS-456 G. Kawahara, S. Kida, M. Tanaka and S. Yanase,
Wrap, Tilt and Stretch of Vorticity Lines around a Strong Straight Vortex Tube in a Simple Shear Flow; Oct. 1996

NIFS-457 K. Itoh, S.- I. Itoh, A. Fukuyama and M. Yagi,
Turbulent Transport and Structural Transition in Confined Plasmas; Oct. 1996

NIFS-458 A. Kageyama and T. Sato,
Generation Mechanism of a Dipole Field by a Magnetohydrodynamic Dynamo; Oct. 1996

NIFS-459 K. Araki, J. Mizushima and S. Yanase,
The Non-axisymmetric Instability of the Wide-Gap Spherical Couette Flow; Oct. 1996

NIFS-460 Y. Hamada, A. Fujisawa, H. Iguchi, A. Nishizawa and Y. Kawasumi,
A Tandem Parallel Plate Analyzer; Nov. 1996

NIFS-461 Y. Hamada, A. Nishizawa, Y. Kawasumi, A. Fujisawa, K. Narihara, K. Ida, A. Ejiri, S. Ohdachi, K. Kawahata, K. Toi, K. Sato, T. Seki, H. Iguchi, K. Adachi, S. Hidekuma, S.Hirokura, K. Iwasaki, T. Ido, M. Kojima, J. Koong, R. Kumazawa, H. Kuramoto, T. Minami, I. Nomura, H. Sakakita, M. Sasao, K.N. Sato, T. Tsuzuki, J. Xu, I. Yamada and T. Watari,
Density Fluctuation in JIPP T-IIU Tokamak Plasmas Measured by a Heavy Ion Beam Probe; Nov. 1996

NIFS-462 N. Katsuragawa, H. Hojo and A. Mase,
Simulation Study on Cross Polarization Scattering of Ultrashort-Pulse Electromagnetic Waves; Nov. 1996

NIFS-463 V. Voitsenya, V. Konovalov, O. Motojima, K. Narihara, M. Becker and B. Schunke,
Evaluations of Different Metals for Manufacturing Mirrors of Thomson Scattering System for the LHD Divertor Plasma; Nov. 1996

NIFS-464 M. Pereyaslavets, M. Sato, T. Shimozuma, Y. Takita, H. Idei, S. Kubo, K. Ohkubo and K. Hayashi,
Development and Simulation of RF Components for High Power Millimeter Wave Gyrotrons; Nov. 1997

NIFS-465 V.S. Voitsenya, S. Masuzaki, O. Motojima, N. Noda and N. Ohyabu,
On the Use of CX Atom Analyzer for Study Characteristics of Ion Component in a LHD Divertor Plasma; Dec. 1996

NIFS-466 H. Miura and S. Kida,
Identification of Tubular Vortices in Complex Flows; Dec. 1996

NIFS-467 Y. Takeiri, Y. Oka, M. Osakabe, K. Tsumori, O. Kaneko, T. Takanashi, E. Asano, T. Kawamoto, R. Akiyama and T. Kuroda,
Suppression of Accelerated Electrons in a High-current Large Negative Ion Source; Dec. 1996

NIFS-468 A. Sagara, Y. Hasegawa, K. Tsuzuki, N. Inoue, H. Suzuki, T. Morisaki, N. Noda, O. Motojima, S. Okamura, K. Matsuoka, R. Akiyama, K. Ida, H. Idei, K. Iwasaki, S. Kubo, T. Minami, S. Morita, K. Narihara, T. Ozaki, K. Sato, C. Takahashi, K. Tanaka, K. Toi and I. Yamada,
Real Time Boronization Experiments in CHS and Scaling for LHD; Dec. 1996

NIFS-469 V.L. Vdovin, T.Watari and A. Fukuyama,
3D Maxwell-Vlasov Boundary Value Problem Solution in Stellarator Geometry in Ion Cyclotron Frequency Range (final report); Dec. 1996